ROLE OF FLAME-EXPANSION WAVE INTERACTIONS ON BURNING RATE ENHANCEMENT AND FLAME ACCELERATION IN HYDROGEN-AIR MIXTURES

Kevin Cheevers[1], Hongxia Yang[2], Andrzej Pekalski[3], Matei Radulescu[4]

[1]**University of Ottawa, Ottawa, Canada, Kevin.Cheevers@uOttawa.ca**
[2]**University of Ottawa, Ottawa, Canada, HYang6@uOttawa.ca**
[3]**Shell Global Solutions UK, London, United Kingdom, Andrzej.Pekalski@Shell.com**
[4]**University of Ottawa, Ottawa, Canada, Matei@uOttawa.ca**

ABSTRACT

Hydrogen flames are much thinner than hydrocarbon flames. They have a higher propensity to wrinkle and are subject to thermo-diffusive instabilities in lean conditions. The large scale experiments of Sherman under partially vented conditions have shown that the transition to detonation is possible with only modest flame acceleration to approximately 200 m/s, which is much lower than the commonly accepted limits corresponding to choked flames. At present, the reason for this transition is not known. Vented H_2-air explosions have also demonstrated the role played by expansion/flame interactions in deforming the flame. The state of the art on flame burning rate enhancement by expansion waves will be provided, along with the recent experimental and numerical results of head on interaction of flames with an expansion wave conducted in our group. We show that the expansion wave interaction can generate local burning rate increases by more than an order of magnitude. The role of thermo-diffusive instability is also assessed. The mechanism of flame deformation is via the vorticity generation by the misaligned pressure gradient controlled by the expansion wave and the density gradient of the flame. Expansion waves originating from the unburned gas severely elongate the cells until the flame folds burn out. Expansion waves originating from the burned gas side first invert the flames, then elongate them by the same mechanism. The rate of elongation is controlled by the volumetric expansion of the gas and the curvature-enhanced growth.

1 INTRODUCTION

Hydrogen-air mixtures are more sensitive to ignition and propagate stronger flames than hydrocarbon mixtures. Detonations in hydrogen-air mixtures have smaller cell sizes, are more easily directly initiated by a strong energy source, and are more difficult to quench. The acceleration of hydrogen-air flames in confined tubes or in the presence of obstructions are also more rapid due to the very thin flames and inability of turbulence to locally quench small scale flame folds. Thermo-diffusive instabilities promote the sustenance of small scale flamelets and further contribute to wrinkling. The flame accelerations in hydrogen mixtures are more likely to transit to detonations, owing the combination of the propensity of the flame to accelerate and the auto-ignition sensitivity of the gas compressed by the flame driven shocks.

Indeed, deflagration to detonation transition (DDT) in hydrogen-air flames has a long history of study in the nuclear industry, where loss-of-coolant type accidents like Fukushima lead to a large production of hydrogen in confined environments. The growing interest and adoption of hydrogen as an energy carrier in the transportation and domestic industry thus raises novel challenges of safety considerations associated with large scale releases and potential flame acceleration in other partially obstructed and vented situations.

Recently, there have been a number of accidents involving hydrogen, such as the accidental venting of hydrogen at a Norwegian hydrogen refuelling station, where detonation of the released fuel-air mixture is suspected to have occurred [1]. This has caused some delays in the deployment of hydrogen technologies in the country, and serves as an example of the price incurred by such incidents.

Studies of flame acceleration and propensity to DDT in hydrogen-air mixtures in large scale partially vented experiments have revealed unsuspected sensitivity to DDT. The large-scale experiments of Sherman with lean hydrogen-oxygen mixtures suggest that transverse venting can be crucial in promoting a detonation transition during flame acceleration [2]. Whereas non-vented experiments in the same study without internal congestion had occasional DDT events located near the end of a 30.5 m tube, the inclusion of a 13% lateral venting area sufficiently enhanced the flame to shorten the DDT distance to approximately 11 m. More surprisingly, the same study reported a transition to detonation when the flame accelerated to only approximately 230 m/s. This speed is much lower than the anticipated speed for a CJ deflagration speed, which is usually the criterion of transition in less sensitive hydrocarbon based fuels [3], and approximately given by the speed of sound in the burned products in strongly confined or closed tubes.

It is currently not clear whether the transition to detonation at such low speed is due to the more sensitive nature of hydrogen auto-ignition. This is unlikely to be the principal cause, as simple estimates of auto-ignition delay times at the corresponding states are simply too long to account for the DDT events. Instead, we conjecture that the local acceleration of these flames is the culprit for the rapid transition to detonation. A program of research has thus been initiated at the University of Ottawa in collaboration with Shell in order to establish the mechanisms for enhanced flame acceleration and potential transition to detonation in hydrogen-air mixtures in flames propagating in vented vessels. We report on the progress of our investigation studying the role of partial venting and rapid depressurization of hydrogen explosions on the flame acceleration.

2 ROLE OF RAPID VENTING ON FLAME DYNAMICS

Flame propagation in vented vessels with impulsive depressurization has been long known to be subjected to rapid deformation of the flame structure [4]. The mechanism at play is the interaction of expansion waves with the flame front.

Rapid depressurization and venting leads to expansion waves. Venting is a common measure of mitigation of explosions to reduce the pressure in a system and minimize damage to equipment, buildings, and occupants [5]. Cooper et al. illustrate well the sequence of events in a vented explosion experiment consisting of the ignition of a flame in a pressure vessel, the bursting of a diaphragm due to the pressure increase in the vessel, and the subsequent venting of the vessel contents to the atmosphere [4]. The rupture of a diaphragm separating the contents of the vessel from the environment, such as a burst disk or blowout panel, is the canonical Riemann problem which results in the generation of a shock wave in the lower-pressure external medium and an expansion wave propagating upstream towards the flame. Depending on the particulars of a vented explosion such as the size of the vent, burst pressure, dimensions of the vessel, and combustive properties of the reactive mixture, additional acoustic waves may be generated during later stages in addition to the initial venting process [6]. Dorofeev has suggested that sudden venting of a pressurized vessel with an active flame could sufficiently enhance the flame to trigger DDT [7].

The burning properties of flames have previously been shown to be sensitive to acoustic wave interactions, which can enhance or diminish the flame [8–10]. Similarly, a large amount of work has been done studying the flame enhancement and acceleration resulting from interactions with shock waves [11–18]. Kilchyk and co-workers numerically studied the interaction of both a shock and an expansion wave with a flame [19]. They found that the strongest flame amplification for shock flame interactions was observed when a shock originates from the product gases. Expansion waves were also shown to increase the flame burning rate, with fresh gas expansion waves offering larger flame enhancement. It was noted that expansion-induced flame enhancement occurs over a longer timespan than shock-flame interactions.

Laviolette [20] proposed an experiment to study expansion wave-flame interactions in propane-oxygen-nitrogen mixtures, which evolves a spherical flame in a vertical tube and rupturing a diaphragm to

generate an expansion wave in the test gas. The flame front itself is greatly distorted by the interaction, and a greater pressure increase is measured in cases with expansion wave interactions. A related work using a more sensitive propane-oxygen-nitrogen mixture and a larger tube showed that the interaction of the flame with an expansion could induce DDT earlier than a flame accelerating without expansion wave-induced enhancement [21].

3 OUR RESEARCH PROGRAM

Recognizing the importance of flame-expansion wave interactions, our current program of study aims to isolate the problem of flame interaction with an expansion wave in various canonical configurations. This includes an expansion wave interacting with a wrinkled flame in which the former originates from the front, back, and laterally via sudden depressurization. We aim to establish the mechanism of flame deformation and develop numerical and scaling models to predict the enhancement of flame burning rate caused by the interaction.

The configuration we study is an improvement of the shock-tube technique of Laviolette. It involves generating a planar wrinkled flame, such that the mechanisms of flame enhancement are most transparent for study. This also removes other effects associated with vented explosion experiments, such as Helmholtz bulk oscillations caused by the sequential bouncing of pressure waves through experimental vessels [22], and the turbulence generated upon initial vent opening [23]. The canonical configuration also allows comparison with numerical models. The configuration extends our previous work on the head-on interaction of wrinkled flames with shock waves [18].

4 THIS PAPER

In the present paper, we report upon the progress we have made on modelling and design of the experimental configuration to study head-on interaction of wrinkled hydrogen-air flames with expansion waves. We aim to establish the mechanism of flame enhancement and the magnitude of the burning rate time history resulting from the interaction, highlighting the role of the direction of the expansion wave (originating from the burned or unburned side of the flame). The mixtures studied are stoichiometric and lean hydrogen-air, in order to also assess the role of thermo-diffusive instabilities in the lean hydrogen flames. We also comment on the role played by the expansion wave gradient, controlled by the distance separating the flame and the expansion wave.

5 NUMERICAL SIMULATION SET-UP

The problem we study in the numerical simulations is that of the head-on interaction between a cellular flame and an expansion wave, as illustrated in Fig. 1. The simulations are conducted in two steps. First, calculations are performed to establish wrinkled flames. These calculations are initialized with the planar laminar flame solution. Small perturbations trigger the cellular instability. The calculations are allowed to run until the flame develops a saturated cellular structure.

The wrinkled flame solutions are then used in separate calculations where the pressure in either the burned or unburned gas is suddenly reduced, and separates the higher pressure zone containing the flame by a numerical planar ”diaphragm”. The sudden release of this diaphragm generates a nominally one-dimensional expansion wave, which then interacts with the wrinkled flame structure.

The problem is studied in a two-dimensional rectangular domain, in which the flame is modelled using the reactive Navier-Stokes equations. The reaction kinetics are modelled using single-step Arrhenius chemistry, tuned to reproduce the desired flame properties. The horizontal domain boundaries use symmetric conditions, whereas the inflow and outflow boundaries are free. The Navier Stokes equations are solved using a second-order accurate Godunov exact Riemann solver for the convective terms and a second-order centred difference scheme for the diffusive terms [24, 25]. The chemistry is evolved through second-order time-stepping. The model’s input parameters are shown in Table 1, calculated for

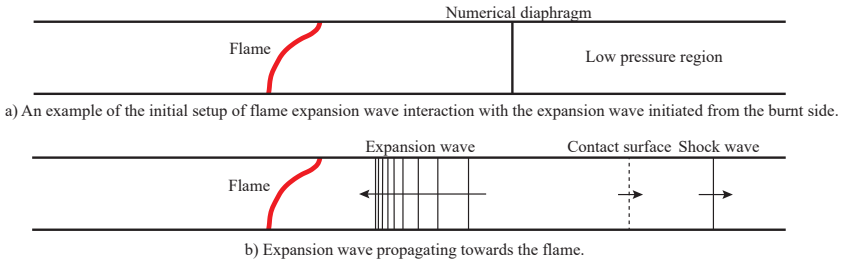

Fig. 1: Sketch of the numerical set-up of the flame-expansion wave interaction.

	ρ_0 (kg/m^3)	S_L (m/s)	$K/(\rho c_p)$ (m^2/s)	L_f (m)	γ	μ (pa s)
ϕ = 1.0	0.1474	1.98	2.60 $\times 10^{-4}$	0.0034	1.4013	1.81 $\times 10^{-5}$
ϕ = 0.5	0.1706	0.76	2.05 $\times 10^{-4}$	0.0031	1.4007	1.82 $\times 10^{-5}$
	E_a/R (K^{-1})	Q (J/kg)	A (s^{-1})	P_r	L_e	ρ_u/ρ_b
ϕ = 1.0	27390	3.00 $\times 10^6$	4.43 $\times 10^{11}$	0.4655	1.0	8.33
ϕ = 0.5	15160	1.72 $\times 10^6$	6.85 $\times 10^9$	0.5205	0.53	5.88

Table 1: Thermo-chemical properties and model parameters for the hydrogen-air mixtures combustion at T=294 K and p_0 = 17.24 kPa.

a stoichiometric ($\phi = 1.0$) and lean ($\phi = 0.5$) hydrogen-air laminar free flame with an initial fresh gas temperature of 294 K and pressure of 17.2 kPa. The procedure for calculating these input parameters and additional details on the numerical framework can be found in Yang & Radulescu [18].

A vertical laminar flame was initially placed in the centre of the rectangular domain, which has a length of 1000 L_{fs} and a height of 16.5 L_{fs}, with the characteristic length scale of the flame $L_{fs} = \frac{K}{\rho_u S_L c_p}$. A small longitudinal perturbation was placed on the flame, from which a cellular flame was evolved. Once the cellular flame has been sufficiently developed, a numerical diaphragm placed at a distance of $L_0 = 141 L_{fs}$ is ruptured to generate an expansion wave. The low pressure region on the other side of the numerical diaphragm has an initial temperature of 294K. The strength of the expansion wave is adjusted by varying the pressure of the low-pressure region, whereas the pressure gradient across the expansion wave is adjusted by varying the distance separating the flame from the numerical diaphragm.

6 EXPERIMENTAL METHOD

A 3.4 m long shock tube with a rectangular cross-section of 203 mm by 19 mm was used for these experiments. A high-pressure test section, initially filled with a hydrogen-air mixture to a maximum pressure of 17.2 kPa, was separated from the low pressure section, initially filled with air, by the use of a diaphragm. A tungsten wire igniter, similar to that used by Yang & Radulescu [18], was installed vertically in the test section. The vertical tungsten wire was used to ignite a flat laminar flame. A series of high-frequency piezoelectric PCB pressure transducers were mounted on the top wall of the shock tube to record pressure histories. Z-type Schlieren photography was used to record the evolution of the flow field over a region of 330 mm by 203 mm with an exposure time of 0.468 μs. A schematic of the shock tube can be seen in Figure 2. To visualize the evolution of the flame in absence of rarefaction waves, the diaphragm was replaced by a solid wall.

Similar to Laviolette, controllably and reproducibly rupturing the diaphragm at low pressures has proven to be very difficult due to the low pressure loading of the diaphragm. This in turn reduces the ability of a puncture in a thin material to amplify into a large tear. An improved solution consisting of a hammer which strikes thin glass diaphragms is currently underway. For these initial experiments, however, a thin 0.03 mm polyethylene film was used to separate the two regions. The flame-induced pressure increase

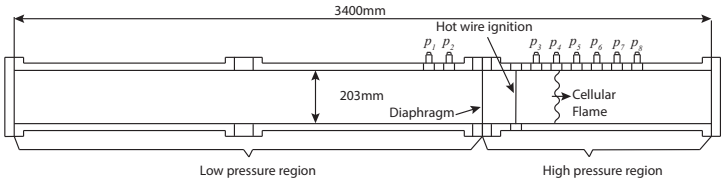

Fig. 2: Illustration of the low-pressure experimental configuration. The tungsten wire igniter is placed at either extremity of the channel, depending on whether the expansion wave is generated in the fresh or product gases. All measurements are in millimetres.

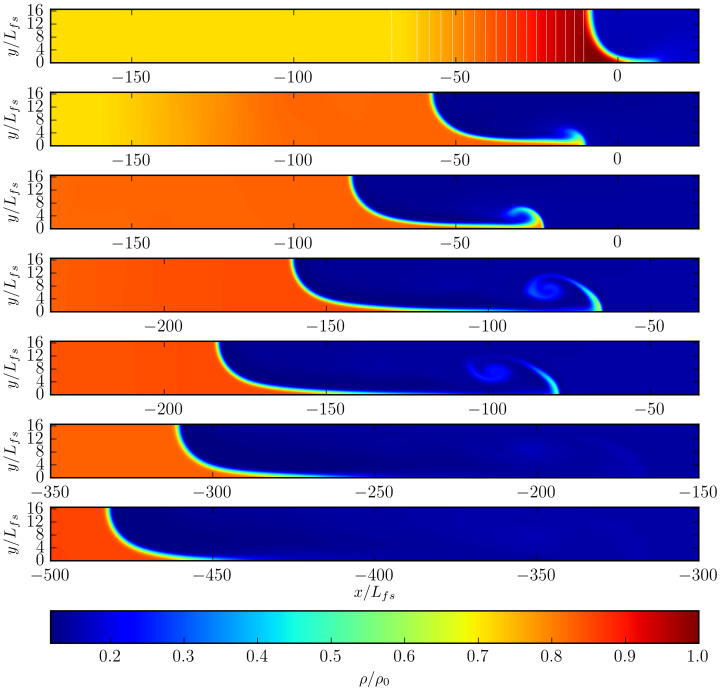

Fig. 3: Density profiles illustrating the interaction of the $\phi = 0.5$ flame and the expansion wave from the fresh gases at times t/t_{fs} = 0 (top), 0.25, 0.35, 0.66, 0.75, 1.25, and 1.92 (bottom). The white lines in the topmost image show the gradient of the expansion wave before the interaction.

in the high-pressure region eventually raises the pressure beyond the film's rupture pressure, causing the generation of the expansion wave during the rupture of the diaphragm.

7 RESULTS

Figure 3 summarizes a typical result obtained for the interaction of a flame with an expansion wave originating from the fresh gases, and shows the mechanisms of flame deformation. Beginning with the interaction of the flame with the fresh gas expansion wave, the topmost image shows the profile of the initial cellular flame and the expansion wave resulting from the rupture of a diaphragm located at a distance of L_0. The following two frames show a significant increase of the flame surface area resulting from the flame-expansion wave interaction as a severe elongation of a funnel, or "spike" of fresh gas. This increase in flame surface area is caused by the vorticity deposition by the baroclinic torque resulting from the misalignment of the flame density gradient and expansion wave pressure gradient, as argued by Laviolette [20]. Further deformation is then enhanced by the combination of gas expansion and thermo-diffusive instabilities. This flame deformation lasts until the flame consumes the gas in the funnel. In Fig. 5a, the time evolution of the flame burning velocity is shown for this interaction, in which the increase in flame surface area manifests as a corresponding increase in flame burning velocity. A peak

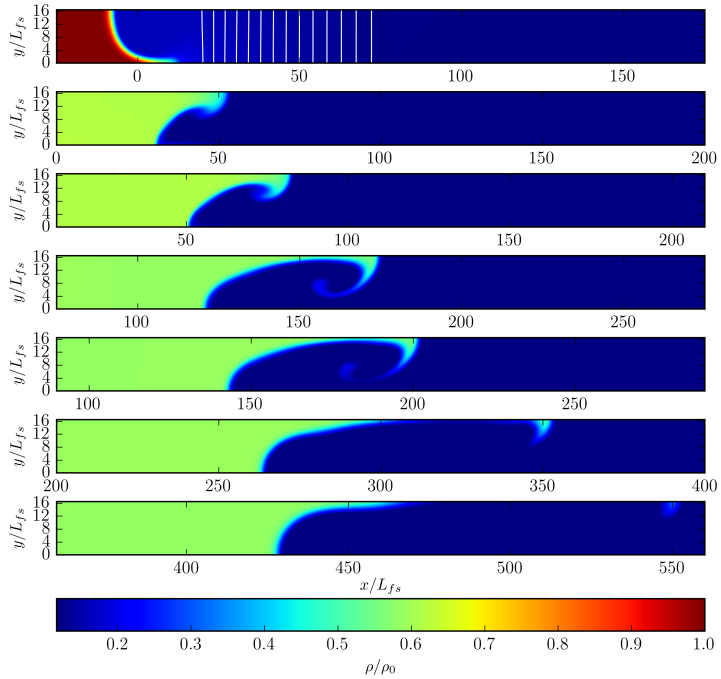

Fig. 4: Density profiles illustrating the interaction of the $\phi = 0.5$ flame and the expansion wave from the product gases at times t/t_{fs} = 0 (top), 0.25, 0.35, 0.66, 0.75, 1.25, and 1.92 (bottom). The white lines in the topmost image show the gradient of the expansion wave before the interaction.

burning velocity 10 times larger than laminar one is reached, after which the burning velocity decreases as the fresh gas in the funnel neck is consumed and the flame surface area decreases. This mechanism of the expansion wave-induced flame enhancement is similar to the shock-flame enhancement mechanisms identified by Yang & Radulescu [18]. The enhancement of flame burning velocity resulting from the interaction with a shock wave the same pressure ratio of 1.6 is also shown in Fig. 5a, following the same trend. The mechanism of flame deformation is similar in both cases, as highlighted by Yang & Radulescu, in that the passage of a pressure wave over the flame deposits vorticity on the latter, which results in an area increase. They describe in detail the multiple phases of flame deformation, however an important feature in such problems is the exponential feedback between the flame surface area and burning rate increases. As a result of the greater thickness and lower propagation speed of an expansion wave when compared to shock waves, the interaction time, and thus vorticity deposition time, is longer than in shock-flame interactions. This results in a higher peak burning velocity.

Figure 4 shows a typical result obtained for the interaction of a cellular flame with an expansion wave originating in the product gases at a distance of L_0 from the flame. The flame initially reverses during the interaction with the expansion wave, caused by the opposite sign of the vorticity deposited on the flame during the interaction. Following this reversal, the flame deforms similarly to the deformation seen following the fresh gas expansion wave interaction, in Fig. 3. This affects the flame burning velocity, shown in Fig. 5a, which exhibits an initial decrease as the flame flattens and reverses. Following the reversal, the flame burning velocity increases before reaching a peak burning velocity which is lower than the peak velocities resulting from the fresh gas expansion-flame interaction and the shock-flame interaction. Additionally, the time elapsed until reaching the peak burning velocity is longer in the product gas expansion-flame interaction than the fresh gas expansion-flame interaction.

The equivalence ratio of the hydrogen-air mixture was varied to practically study stoichiometric and lean flames. Lowering the equivalence ratio results a competition between the flame enhancement caused by additional wrinkling stemming from the increase of thermo-diffusive instabilities at lower Lewis numbers, but also the weakening of the flame caused by lower Darrieus-Landau instabilities stemming

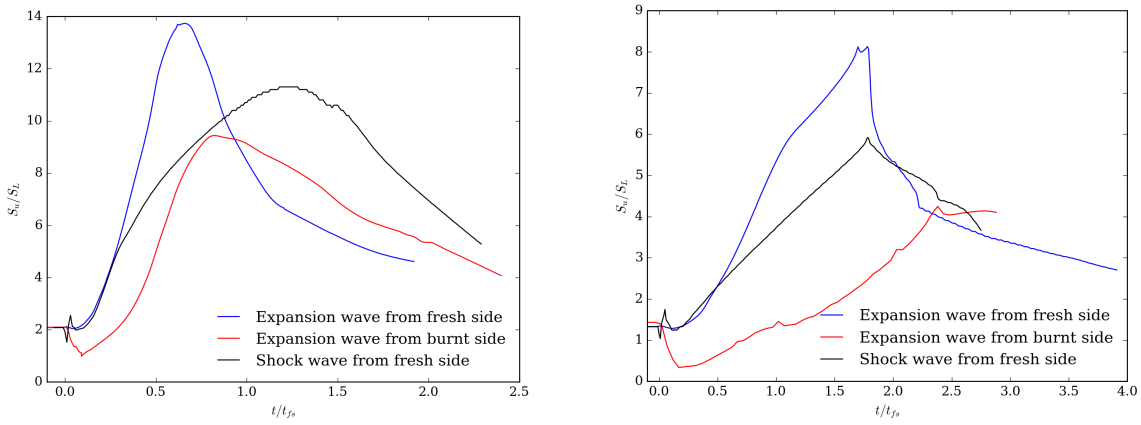

(a) $\phi = 0.5$ (b) $\phi = 1.0$

Fig. 5: Time evolution of the burning velocity of lean ($\phi = 0.5$) and stoichiometric ($\phi = 1.0$) hydrogen-air flames after the interaction with an expansion or shock wave with a pressure ratio of 1.6.

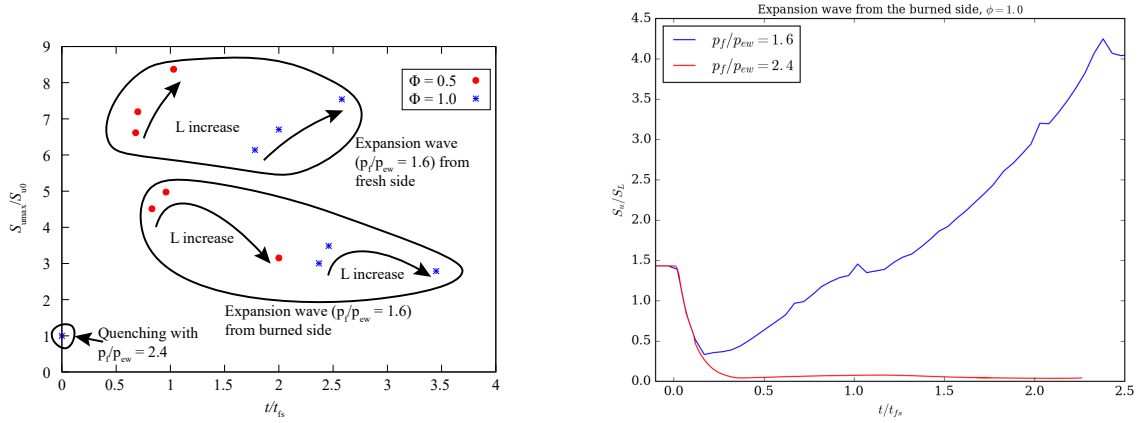

(a) (b)

Fig. 6: a) Summary of the maximum flame burning velocity as a function of time, for increasing initial separation of the flame and the diaphragm. b) Evolution of the flame burning velocity for expansion waves originating at L_0 in a $\phi = 1.0$ mixture, with varying pressure ratios.

from its lower expansion ratio. When considering only the lower expansion ratio across the flame, one would expect the maximum burning velocity attained by the lean flame to be smaller than that of the stoichiometric flame from neglecting the Lewis number effects. However, Figure 5 shows that the maximum burning velocity of the lean flame is 75% - 100% higher than the peak burning velocity of the stoichiometric flame, which emphasizes the importance of the additional wrinkling of the flame in enhancing the flame. Thus, lower equivalence ratios result in larger peak burning velocities as thermo-diffusive instabilities dominate.

The effect on the pressure gradient has also been studied by varying the initial distance separating the cellular flame and the diaphragm from L_0 to $1.5L_0$ and $5L_0$. Increasing the distance initially separating the flame from the diaphragm will result in shallower pressure gradients across the wave. Longer distances from the flame to the expansion wave in the fresh gases leads to a negligible effect on flame deformation, as the residence time of the vorticity deposition and the rate of vorticity deposition balance such that the total vorticity deposited remains the same. However, thicker waves provide slightly more wave enhancement. This can be seen in Fig. 6a, which shows a very weak increase in peak burning velocities provided the expansion originates in the fresh gases. In contrast, increasing the distance between the flame and the diaphragm when the latter is located in the product gases has a stronger effect on the

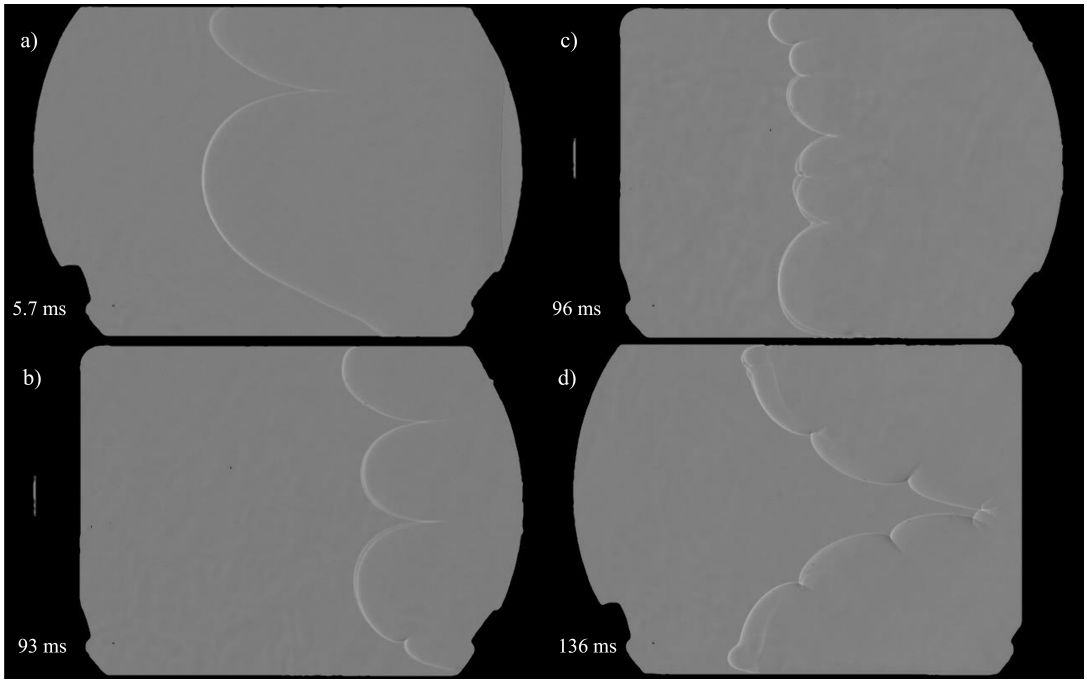

Fig. 7: Experimental frames showing the ignition and propagation of the flame, with timestamps taken from the moment of first ignition at the centre of the wire. The field of view changes between frames to show the flame evolution throughout the tube.

flame's peak burning velocity. This is a result of the negative phase of the flame reversal and non-linear effects reducing the small-scale flame deformation.

The interaction of a flame with a stronger expansion wave whose pressure ratio was 2.4, originating from the product gases, was studied. Despite a small initial increase in flame amplitude after the interaction, the burning velocity evolved towards a very small, near-zero value, as shown in Fig. 6b. This suggests that a sufficiently strong expansion originating from the product gases may quench the flame rather than enhance it due to cooling during the initial flame reversal stage. While the flame weakens, local flamelets can be extinguished by excessive strain rates.

8 EXPERIMENTAL RESULTS

The initiation and propagation of a flame in a mixture of $2H_2 + O_2 + 3.76N_2$ with an initial pressure and temperature of 17.2 kPa and 294 K is shown in Fig. 7. The flame is ignited at multiple points along the tungsten wire, and initially propagates through the channel with two large cells. Soon thereafter, the flame evolves to a flat cellular flame and continues propagating in this mode. The flame periodically generates more cells as it flattens, resulting in a vertical wrinkled flame in the second and third frames. After having passed the halfway point, the flame begins evolving into a tulip flame until reaching the end wall. The generated flame is deemed to be sufficiently flat in these intermediate frames for these experiments, and qualitatively resembles the flame generated by Yang & Radulescu to study shock-flame interactions [18]. The flame initiation and initial flame growth is very reproducible between subsequent experiments.

Flame-expansion wave interaction experiments were also performed, with a typical experiment shown in Fig. 7. A flame initially propagates from right to left through the first three frames with an average speed around 16 m/s, when measured along the top wall. At much later times, after the rupture of the diaphragm on the product side of the flame, the flame is seen propagating through the field-of-view in the opposite direction at a speed around 91 m/s. In the last three frames, one sees the flame deformation caused by the interaction with the expansion wave, including the reversal of both the small-

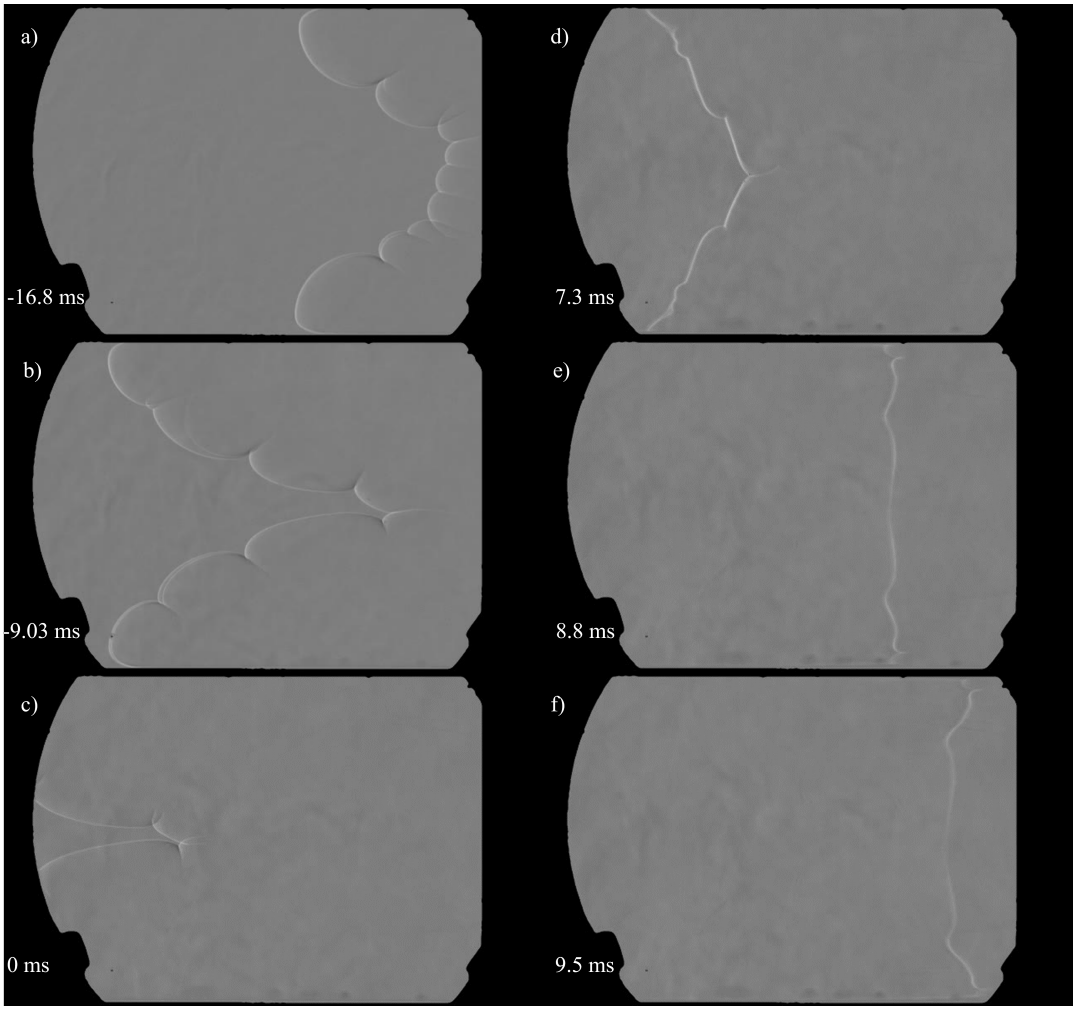

Fig. 8: Low-pressure experiments, with a reactive gas pressure of 17.2 kPa and an inert gas pressure of 1.7 kPa, for a pressure ratio of 10. A wrinkled flame propagates from right to left through the frame at an average velocity around 16 m/s when measured along the top wall. The flame is seen propagating across the field of view at a velocity around 91 m/s due to the expansion-driven flow acceleration. The reversal of flame features of all scales is seen in the right-hand images.

scale features and the macroscopic tulip flame, suggesting a global reversal of all the features of the flame resulting from this interaction. However, the longer timescales involved with the tulip flame reversal prevents further investigation due to the presence of the reflected waves in the shock tube. New experimental apparatus is currently under construction to increase the experimental time window relative to the characteristic interaction time and study the later stages of the tulip flame reversal.

9 CONCLUSIONS

The enhancement of a cellular flame resulting from the interaction with an expansion wave was studied in numerical experiments with lean and stoichiometric hydrogen-air flames. The deposition of vorticity on the flame by baroclinic torque was identified as the flame deformation mechanism, enhanced by later thermo-diffusive instabilities. The peak flame burning velocity resulting from the interaction of a flame with a fresh gas expansion waves was shown to exceed that caused by shock-flame interactions, whereas the initial reversal of the flames during the interaction of a flame with a product gas expansion wave reduces the efficiency of the flame enhancement, resulting in lower peak burning velocities. In lean low equivalence ratio mixtures, the increased importance of thermo-diffusive instabilities outweighs the reduced expansion ratio. As a consequence, a net increase of the peak burning velocity with decreasing

equivalence ratio was identified. The thickness and pressure gradient of the expansion wave was found to have a minimal effect on the peak burning velocity when propagating from the fresh gases, however these parameters become important when the expansion wave originates in the burned gas. This stems from the initial flame reversal during interaction with product gas expansion waves and non-linear effects which reduce small-scale deformations. Finally, the strength of the expansion wave originating in the product gases was increased and suggested a pathway to expansion-induced flame quenching which relies on providing sufficient cooling during the flame reversal to overcome feedback effects caused by flame surface area increases after the reversal.

An experimental method was proposed to study the interaction of a planar expansion wave and a flame at low pressures. A flat laminar flame was ignited by the tungsten wire igniter and evolved into a wrinkled flame as it propagated through the channel. Preliminary experiments have shown the flame reversal featured in the numerical work when expansion waves are generated in the product gas. Notably, observations of the reversal of flame features at all scales were presented, including the flattening and reversal of a channel-height tulip flame. Despite this, the flame enhancement cannot yet be quantified. Improvements to the experimental setup, particularly the reproducibility and control of diaphragm rupture mechanism and increasing the experimental time window are ongoing and remain a requirement prior to experimentally quantifying the flame enhancement.

Our numerical experiments suggest that very large deformations of the wrinkled flame structure are expected in the presence of transient expansion waves. These were found to be larger than the burning rate enhancement produced by shock waves with same absolute value of pressure jump. These punctuated large enhancements of burning rate may thus explain why DDT events may appear during rapid depressurization of vented explosions of sufficiently large scales. Clearly, future work should address phenomena at larger scales, where turbulent local flame speeds may approach high enough values to bring coupling between the flame-generated turbulence [26, 27] and auto-ignition phenomena in the gases compressed by the flame acceleration.

References

[1] O. R. Hansen, "Hydrogen infrastructure—efficient risk assessment and design optimization approach to ensure safe and practical solutions," *Process Safety and Environmental Protection*, vol. 143, pp. 164–176, 2020.

[2] M. P. Sherman, S. R. Tieszen, and W. B. Benedick, "Flame facility: The effect of obstacles and transverse venting on flame acceleration and transition on detonation for hydrogen-air mixtures at large scale,"

[3] W. Rakotoarison, *Chapman-Jouguet Deflagration and their Transition to Detonations*. PhD thesis, University of Ottawa, 2023.

[4] M. Cooper, M. Fairweather, and J. Tite, "On the mechanisms of pressure generation in vented explosions," *Combustion and Flame*, vol. 65, no. 1, pp. 1–14, 1986.

[5] *NFPA 68: Standard on explosion protection by deflagration venting*. 2023.

[6] K. Yang, Q. Hu, S. Sun, P. Lv, and L. Pang, "Research progress on multi-overpressure peak structures of vented gas explosions in confined spaces," *Journal of Loss Prevention in the Process Industries*, vol. 62, p. 103969, Nov. 2019.

[7] S. Dorofeev, A. Bezmelnitsin, and V. Sidorov, "Transition to detonation in vented hydrogen-air explosions," *Combustion and Flame*, vol. 103, no. 3, 1995.

[8] W. Kaskan, "An investigation of vibrating flames," *Symposium (International) on Combustion*, vol. 4, no. 1, pp. 575–591, 1953. Fourth Symposium (International) on Combustion.

[9] G. Searby, "Acoustic instability in premixed flames," *Combustion Science and Technology*, vol. 81, pp. 221–231, Feb. 1992.

[10] J. Yanez, M. Kuznetsov, and J. Grune, "Flame instability of lean hydrogen–air mixtures in a smooth open-ended vertical channel," *Combustion and Flame*, vol. 162, pp. 2830–2839, July 2015.

[11] G. Markstein, *Nonsteady Flame Propagation*. AGARD graph, Pergamon Press, 1964.

[12] A. Khokhlov, E. Oran, and G. Thomas, "Numerical simulation of deflagration-to-detonation transition: the role of shock–flame interactions in turbulent flames," *Combustion and Flame*, vol. 117, no. 1, pp. 323–339, 1999.

[13] A. M. Khokhlov, E. S. Oran, A. Y. Chtchelkanova, and J. Wheeler, "Interaction of a shock with a sinusoidally perturbed flame," *Combustion and Flame*, vol. 117, no. 1, pp. 99–116, 1999.

[14] G. Thomas, R. Bambrey, and C. Brown, "Experimental observations of flame acceleration and transition to detonation following shock-flame interaction," *Combustion Theory and Modelling*, vol. 5, pp. 573–594, Dec. 2001.

[15] G. Ciccarelli, C. T. Johansen, and M. Parravani, "The role of shock–flame interactions on flame acceleration in an obstacle laden channel," *Combustion and Flame*, vol. 157, no. 11, pp. 2125–2136, 2010.

[16] H. Wei, D. Gao, L. Zhou, D. Feng, and R. Chen, "Different combustion modes caused by flame-shock interactions in a confined chamber with a perforated plate," *Combustion and Flame*, vol. 178, pp. 277–285, 2017.

[17] W. Rakotoarison, B. Maxwell, A. Pekalski, and M. I. Radulescu, "Mechanism of flame acceleration and detonation transition from the interaction of a supersonic turbulent flame with an obstruction: Experiments in low pressure propane–oxygen mixtures," *Proceedings of the Combustion Institute*, vol. 37, no. 3, pp. 3713–3721, 2019.

[18] H. Yang and M. I. Radulescu, "Dynamics of cellular flame deformation after a head-on interaction with a shock wave: reactive richtmyer–meshkov instability," *Journal of Fluid Mechanics*, vol. 923, p. A36, 2021.

[19] V. Kilchyk, R. Nalim, and C. Merkle, "Laminar premixed flame fuel consumption rate modulation by shocks and expansion waves," *Combustion and Flame*, vol. 158, no. 6, pp. 1140–1148, 2011.

[20] J.-P. Laviolette, "Experimental investigation of flamerarefaction interactions," 2004.

[21] J.-P. Laviolette, A. J. Higgins, and J. H. Lee, "Interaction between a flame and a rarefaction," *Proc. of the 19th ICDERS*, 2003.

[22] D. McCann, G. Thomas, and D. Edwards, "Gasdynamics of vented explosions part i: Experimental studies," *Combustion and Flame*, vol. 59, no. 3, pp. 233–250, 1985.

[23] V. Molkov, A. Grigorash, R. Eber, and D. Makarov, "Vented gaseous deflagrations," *Journal of Hazardous Materials*, vol. 116, pp. 1–10, Dec. 2004.

[24] S. Falle, J. Giddings, K. Morton, and M. Baines, "Numerical methods for fluid dynamics 4," 1993.

[25] B. Maxwell, A. Pekalski, and M. Radulescu, "Modelling of the transition of a turbulent shock-flame complex to detonation using the linear eddy model," *Combustion and Flame*, vol. 192, pp. 340–357, 2018.

[26] M. Saif, W. Wang, A. Pekalski, M. Levin, and M. I. Radulescu, "Chapman–jouguet deflagrations and their transition to detonation," *Proceedings of the Combustion Institute*, vol. 36, no. 2, pp. 2771–2779, 2017.

[27] A. Y. Poludnenko, J. Chambers, K. Ahmed, V. N. Gamezo, and B. D. Taylor, "A unified mechanism for unconfined deflagration-to-detonation transition in terrestrial chemical systems and type ia supernovae," *Science*, vol. 366, no. 6465, p. eaau7365, 2019.